UC Irvine
UC Irvine Previously Published Works

Title
A framework for linking resting-state chronnectome/genome features in schizophrenia: A pilot study.

Permalink
https://escholarship.org/uc/item/9f21g707

Authors
Rashid, Barnaly
Chen, Jiayu
Rashid, Ishtiaque
et al.

Publication Date
2019

DOI
10.1016/j.neuroimage.2018.10.004

Peer reviewed

eScholarship.org Powered by the California Digital Library
University of California

Author Manuscript

Author Manuscript

Author Manuscript

Author Manuscript

HHS Public Access

Author manuscript

Neuroimage. Author manuscript; available in PMC 2020 January 01.

Published in final edited form as:

Neuroimage. 2019 January 01; 184: 843–854. doi:10.1016/j.neuroimage.2018.10.004.

A Framework for Linking Resting-state Chronnectome/Genome Features in Schizophrenia: A Pilot Study

Barnaly Rashid[1,2,*], **Jiayu Chen**[2], **Ishtiaque Rashid**[3], **Eswar Damaraju**[2,4], **Jingyu Liu**[2], **Robyn Miller**[2], **Oktay Agcaoglu**[2], **Theo G. M. van Erp**[5], **Kelvin O. Lim**[6], **Jessica A. Turner**[2,7], **Daniel H. Mathalon**[8,9], **Judith M. Ford**[8,9], **James Voyvodic**[10], **Bryon A. Mueller**[6], **Aysenil Belger**[11], **Sarah McEwen**[12], **Steven G. Potkin**[13], **Adrian Preda**[13], **Juan R. Bustillo**[14], **Godfrey D. Pearlson**[15,16,17], and **Vince D. Calhoun**[2,4,*]

[1]Harvard Medical School, Boston, Massachusetts, USA

[2]The Mind Research Network & LBERI, Albuquerque, New Mexico, USA

[3]Department of Internal Medicine, School of Medicine, University of New Mexico, Albuquerque, New Mexico, USA

[4]Department of Electrical and Computer Engineering, University of New Mexico, Albuquerque, New Mexico, USA

[5]Clinical Translational Neuroscience Laboratory, Department of Psychiatry and Human Behavior, University of California Irvine, Irvine, 92617, CA, USA

[6]Department of Psychiatry, University of Minnesota, Minneapolis, MN, United States

[7]Departments of Psychology and Neuroscience, Georgia State University, Atlanta, GA, 30302, USA

[8]Department of Psychiatry, Weill Institute for Neurosciences, University of California, San Francisco, San Francisco, CA, 94143, United States

[9]Veterans Affairs San Francisco Healthcare System, San Francisco, CA, 94121, United States

[10]Brain Imaging and Analysis Center, Duke University Medical Center, Durham, NC, 27710, United States

[11]Department of Psychiatry, University of North Carolina at Chapel Hill, Chapel Hill, NC, 27599, United States

[12]Department of Psychiatry, University of California, San Diego, La Jolla, CA, 92093, United States

[13]Department of Psychiatry, University of California Irvine, Irvine, CA, 92617, United States

[*]**Corresponding authors**: Vince Calhoun (vcalhoun@mrn.org), Barnaly Rashid (barnaly_rashid@hms.harvard.edu).

Publisher's Disclaimer: This is a PDF file of an unedited manuscript that has been accepted for publication. As a service to our customers we are providing this early version of the manuscript. The manuscript will undergo copyediting, typesetting, and review of the resulting proof before it is published in its final citable form. Please note that during the production process errors may be discovered which could affect the content, and all legal disclaimers that apply to the journal pertain.

Author Manuscript Author Manuscript Author Manuscript Author Manuscript

[14]Departments of Psychiatry & Neuroscience, University of New Mexico, Albuquerque, NM, 87131, United States

[15]Olin Neuropsychiatry Research Center - Institute of Living, Hartford, CT, USA

[16]Department of Psychiatry, Yale University School of Medicine, New Haven, CT, USA

[17]Department of Neurobiology, Yale University School of Medicine, New Haven, CT, USA

Abstract

Multimodal, imaging-genomics techniques offer a platform for understanding genetic influences on brain abnormalities in psychiatric disorders. Such approaches utilize the information available from both imaging and genomics data and identify their association. Particularly for complex disorders such as schizophrenia, the relationship between imaging and genomic features may be better understood by incorporating additional information provided by advanced multimodal modeling. In this study, we propose a novel framework to combine features corresponding to functional magnetic resonance imaging (functional) and single nucleotide polymorphism (SNP) data from 61 schizophrenia (SZ) patients and 87 healthy controls (HC). In particular, the features for the functional and genetic modalities include dynamic (i.e., time-varying) functional network connectivity (dFNC) features and the SNP data, respectively. The dFNC features are estimated from component time-courses, obtained using group independent component analysis (ICA), by computing sliding-window functional network connectivity, and then estimating subject specific states from this dFNC data using a k-means clustering approach. For each subject, both the functional (dFNC states) and SNP data are selected as features for a parallel ICA (pICA) based imaging-genomic framework. This analysis identified a significant association between a SNP component (defined by large clusters of functionally related SNPs statistically correlated with phenotype components) and time-varying or dFNC component (defined by clusters of related connectivity links among distant brain regions distributed across discrete dynamic states, and statistically correlated with genomic components) in schizophrenia. Importantly, the polygenetic risk score (PRS) for SZ (computed as a linearly weighted sum of the genotype profiles with weights derived from the odds ratios of the psychiatric genomics consortium (PGC)) was negatively correlated with the significant dFNC component, which were mostly present within a state that exhibited a lower occupancy rate in individuals with SZ compared with HC, hence identifying a potential dFNC imaging biomarker for schizophrenia. Taken together, the current findings provide preliminary evidence for a link between dFNC measures and genetic risk, suggesting the application of dFNC patterns as biomarkers in imaging genetic association study.

Keywords

Multimodal analysis; resting-state fMRI; schizophrenia; single nucleotide polymorphism; dynamic functional connectivity; parallel ICA

1. INTRODUCTION

Understanding how genetic risk factors are translated into clinical symptoms, disease progression and response to treatment of complex mental disorders, such as schizophrenia

Author Manuscript Author Manuscript Author Manuscript Author Manuscript

(SZ), is challenging. SZ is a serious, highly heritable (i.e. proportion of variance explained by genetic factors; SZ heritability rate is about 80% (Sullivan et al., 2003)) genetically complex disorder with disruptions in brain structure and function, and cognition (Ellison-Wright and Bullmore, 2010; Keshavan et al., 2011; Lichtenstein et al., 2009; Meda et al., 2012). Family and twin studies have shown evidence of moderate to high heritable component related to most psychiatric disorders (Kendler and Eaves,2005). The concordance rate is defined by the probability that a second twin will progress to a disorder given the first examined twin already has the disorder, and for monozygotic twins it has been found to be about 40%−50% for schizophrenia (Cardno and Gottesman, 2000). These results indicate that the unaffected twins might carry a heritable genetic risk for schizophrenia without expressing the disease.

An efficient strategy to unravel the genetic risk factors of SZ is through investigating the effects of genetic variations on intermediate phenotypes such as aberrant brain structure and function, as they are more related to biological mechanisms compared to behavioral measures. An intermediate phenotype or so-called “endophenotype” represents more biologically defined levels, such as cellular, neuronal level or neurocognitive measures, and is thought to reflect the genetic effects more prominently than disease entities such as SZ (Gottesman and Gould, 2003; Gottesman and Shields, 1972). Brain function measured by fMRI data has been proposed as an intermediate phenotype for genetic studies of mental illness, and patients with psychiatric disorders indeed present brain structural and functional idiosyncrasies, which may underlie the clinical manifestations. Such brain related idiosyncrasies in psychiatric disorders include significantly less gray matter and abnormal regional activations during cognitive task performance (Harris et al., 2006; Ivleva et al., 2012; Manoach et al., 2000; Monks et al., 2004). Moreover, disrupted patterns in resting state inter-network functional connectivity have been reported in a wide range of psychiatric disorders, including schizophrenia and bipolar disorder (Bassett et al., 2012; Calhoun et al., 2012; Jafri et al., 2008; Manoliu et al., 2013; Meda et al., 2012; Pearlson and Calhoun, 2009; Rashid et al., 2014), Alzheimer’s disease and mild cognitive impairment (Petrella et al., 2011) and dyslexia (Koyama et al., 2010). Interestingly, studies have suggested that resting state networks are heritable (Fu et al., 2015; Glahn et al., 2010). Further, a recent study on the UK Biobank participants suggested lower rate of heritability for connectivity edges, but higher heritability for independent component analysis (ICA) extracted connectivity components (Elliott et al.,2017). In particular, the default-mode network connectivity was reported to have a heritability of 0.42 (Glahn et al., 2010).

Recent resting state and task-based fMRI studies examining dynamic (i.e., time-varying) functional network connectivity (dFNC) offer additional information beyond conventional, static or average functional network connectivity (sFNC) (Calhoun et al., 2014; Hutchison et al., 2013; Preti et al., 2017; Rashid et al., 2016). The time-varying or dFNC approach focuses on identifying whole brain transient and recurring patterns in temporal coupling in the human brain (Allen et al., 2014; Calhoun et al., 2014; Rashid et al., 2014). The temporal dynamics of the identified components’ timecourses are commonly characterized by the sliding window approach to estimate the connectivity as moving between stable dFNC patterns or states (Allen et al., 2014; Sakoglu et al., 2010). These dFNC states have been shown to be stably present in the data, reoccurring over time, and disrupted by null models,

Author Manuscript Author Manuscript Author Manuscript Author Manuscript

providing further evidence of replicability of dFNC states (Abrol et al., 2016; Abrol et al., 2017; Miller et al., 2017).

Before the availability of low-cost genomic technologies, most genetic association studies focused on exploring candidate genes involvement in a target disease. The advance in technologies has made it possible to study the whole genome, a large portion of which have not been previously studied or understudied for a particular disease (Hirschhorn and Daly, 2005) and therefore, offers substantial potential for identifying cluster of genetic variants associated with complex genetic disorders (Hindorff et al., 2009). The conventional SNP or candidate gene analysis using predefined reference set of SNPs or genes only investigates the SNPs (or genes) of interest. Therefore, it cannot provide a comprehensive genetic risk profile for a complex trait like SZ. Genome-wide association studies (GWAS) can solve this problem, however, it will not shed light on the interplay among genetic variables unless additional analysis (e.g., pathway analysis) is employed for interpretation.

There has been a tremendous growth of interest in the application of multivariate, multimodal techniques, in areas such as imaging-genetics, to understand interactions between neuronal and genetic mechanisms of schizophrenia. The complexity of the genetics in schizophrenia strongly supports a genomic approach, i.e. an approach that can capture not only a single genetic effect but also the relationship between multiple genetic factors and phenotypic information. Imaging genomics method integrates genetic with structural and functional neuroimaging data to explore individuals with multiple genetic risk variants that relate to a psychiatric disorder. Multivariate multimodal techniques provide additional statistical power by extracting genetic and imaging data to capture the aggregated effect of multiple genetic factors and brain regions and assess the co-varying pattern of these data modalities (Calhoun and Sui, 2016; Chen et al., 2013; Liu and Calhoun, 2014). Multivariate data fusion techniques enable us to assess multiple variables simultaneously, and offer some additional benefits over the use of univariate techniques. The interpretation of results from multivariate data-fusion approaches is relatively simple due to co-varying nature of the variables (i.e., regions of interest or ROIs) as measures from patterns are explored rather than a huge number of univariate paired relationships (Calhoun and Sui, 2016). Further, using multivariate strategy replicability of the results can be improved. A number of multivariate data-fusion approaches have been proposed including parallel independent component analysis (pICA) (Liu et al., 2009; Pearlson et al., 2015), joint independent component analysis (jICA) (Calhoun et al., 2006), multiset canonical correlation analysis (mCCA) (Correa et al., 2007), partial least squares (PLS) (Chen et al., 2009), linked ICA (Groves et al., 2011), and coefficient constrained ICA (CC-ICA) (Sui et al., 2009).

The pICA approach, a data-driven technique, is constructed upon the conventional ICA algorithm to jointly conduct separate multivariate analysis in two different data modalities while also optimizing the inter-modality association (Liu and Calhoun, 2014).pICA has been applied to incorporate genetic and neuroimaging data including gray matter density, gray matter volume, and task-related activation (Gupta et al., 2014; Meda et al., 2014; Pearlson et al., 2015). In the context of imaging-genetics study, pICA uses higher order statistics to identify the independent brain networks, associated genetic variants, and their interrelationships (Jagannathan et al., 2010; Liu et al., 2009). Similar to the conventional

Author Manuscript Author Manuscript Author Manuscript Author Manuscript

ICA approach, pICA can identify hidden linear mixture of factors within the genetic and neuroimaging data, while also eliminating unwanted artifacts from the data. The results from the pICA provide independent components (ICs) from both data sets (neuroimaging and genetics) that are inter-linked while maximizing the linkage function in a joint estimation approach (Liu et al., 2009; Meda et al., 2010). There are three criteria that pICA optimizes simultaneously, including identifying a set of maximally independent functional neuroimaging factors, identifying a set of maximally independent genetic variants, and identifying the inter-modality linking relationship between the identified genetic and neuroimaging components. Furthermore, pICA also provides loading parameters for each component that reflect the component's influence in individual subjects (Liu et al., 2009), and interrelationships between neuroimaging and genetic components can be statistically tested and compared between groups.

In the current work, we studied 61 SZ patients and 87 healthy controls with genome-wide single nucleotide polymorphism (SNP) and fMRI data following denoising and quality control (QC) assessment (where SNP data went through several QC steps, imputation and post-imputation QC steps as described in **section 2.2** and Figure S1, and fMRI data went through pre- and post-processing steps as described in **section 2.3** and Figure S2 to ensure data quality). We focused on feature based fusion analysis of an array of genetic variants (SNP) and functional (fMRI) images hypothesizing a significant correspondence between genomic factors and brain function. Our expectation is that the relationship between SNP patterns and time-varying functional connectivity is a more natural way to analyze the data which will improve our understanding of both genomic factors and functional connectivity measures. We estimate the functional features for neuroimaging data as subject-specific states that are revealed from the dynamic FNC data using a sliding window plus clustering approach (Allen et al., 2014; Rashid et al., 2014; Sakoğlu et al., 2010). The SNP data were first pre-filtered using results from an independent GWAS study to locate risk variants based on a large cohort. These risk loci were then simultaneously analyzed for multivariate associations with the derived functional features from fMRI data using the pICA data fusion algorithm. Further, we explored the association between genetic risk and SNP and functional connectivity features. Polygenic risk score (PRS) estimates the aggregate risk of a set of SNPs, by computing a linearly weighted sum of the genetic data where weights are derived from the effect sizes of the individual SNPs obtained from univariate analysis. This approach enables us to study genomic patterns grouped that co-vary across subjects with maximally independent dynamic FNC patterns. To guard against overfitting, the identified dFNC-SNP associations were evaluated with a permutation test.

2. MATERIALS AND METHODS

2.1 Participants

We used resting-state functional magnetic resonance imaging (fMRI) data and single nucleotide polymorphism (SNP) data obtained from 87 healthy controls (61 males, 26 females; mean age 36.83) and 61 age- and gender matched patients with SZ (52 males, 9 females; mean age 38.36) during eyes closed condition as part of the multi-site fBIRN

Author Manuscript Author Manuscript Author Manuscript Author Manuscript

project (Potkin and Ford, 2008). Informed consent was obtained from each participant prior to scanning in accordance with the Internal Review Boards of corresponding institutions.

2.2 SNP Data Preprocessing and Feature Selection

DNA was extracted from blood and saliva samples collected from the participants. No significant difference was noted in genotyping call rates between blood and saliva samples. DNA extraction was performed at the University of California at Irvine and genotyping was performed by Illumina (SD) using a custom made assay including the Infinium MEGA^{ex} chip as well all SNPs on the Psych chip. The SNP data went through quality control (QC), imputation and post-imputation QC as described in (Chen et al.,2018), which is briefly summarized here. PLINK (Purcell et al., 2007) was employed for pre- and post-imputation QC (Chen et al., 2012), including: (a) gender consistency check, (b) sample relatedness (not closer than second degree relatives), (c) genotyping call rate (>90% at both the individual and SNP level), (d) Hardy-Weinberg equilibrium in the control population ($p < 1 \times 10^{-6}$), (e) minor allele frequency (MAF > 0.05). Then imputation was conducted with SHAPEIT used for pre-phasing (Delaneau et al., 2011), IMPUTE2 for imputation (Marchini and Howie, 2010), and the 1000 Genomes data as the reference panel (Altshuler et al., 2012). Only markers with high imputation qualities (INFO score > 0.95) were retained. Missing calls were replaced using high linkage disequilibrium (LD) loci if available or otherwise removed. A total of 977,242 SNP loci were obtained after post-imputation QC and LD pruning ($r^2 < 0.9$), and discrete numbers were then assigned to the categorical genotypes: 0 (no minor allele), 1 (one minor allele), and 2 (two minor alleles). Population structure was corrected with PCA (Price et al.,2006). A pre-filtering (i.e., pre-selection) step was conducted leveraging the Psychiatric Genomic Consortium SZ GWAS (Ripke et al., 2014) based on SZ relevance (i.e., the p- values reported by the PGC SZ GWAS). This resulted in a total of pre-filtered 1546 SNPs, discriminating patients from controls via a univariate SNP-wise test with p-values less than 5×10^{-7} in the GWAS.

Imaging data processing and feature selection

2.3.1 fMRI Data Collection and Preprocessing—Imaging data was collected on 3T Siemens Tim Trio Systems (all but one site) or on a 3T General Electric Discovery MR750 scanner. Resting state fMRI scans were acquired using a standard gradient-echo echo planar imaging paradigm: FOV of 220 × 220 mm (64 × 64 matrix), TR = 2 s, TE = 30 ms, FA = 77°, 162 volumes, 32 sequential ascending axial slices of 4 mm thickness and 1 mm skip. Subjects had their eyes closed during the resting state scan.

Data processing was performed using a combination of toolboxes (AFNI, SPM, GIFT) and custom code written in Matlab. We performed rigid body motion correction using the INRIAlign (Freire and Mangin, 2001) toolbox in SPM to correct for subject head motion followed by slice-timing correction to account for timing differences in slice acquisition.

Then the fMRI data were despiked using AFNI's 3dDespike algorithm to mitigate the impact of outliers. The fMRI data were subsequently warped to a Montreal Neurological Institute (MNI) template (Calhoun et al., 2017), and resampled to 3 mm^3 isotropic voxels. Instead of Gaussian smoothing, we smoothed the data to 6 mm full width at half maximum

Author Manuscript Author Manuscript Author Manuscript Author Manuscript

(FWHM) using AFNI3s BlurToFWHM algorithm, which performs smoothing by a conservative finite difference approximation to the diffusion equation. This approach has been shown to reduce scanner specific variability in smoothness providing a "smoothness equivalence" to data across sites (Friedman et al., 2006). Each voxel time course was variance normalized by removing the mean and dividing by the standard deviation at each voxel prior to performing group independent component analysis as this has shown to better decompose subcortical sources in addition to cortical networks. Note that, no significant group difference in signal-to-noise ratio (SNR) was found (p=0.5, Figure S4).

2.3.2 Group ICA, Intrinsic Connectivity Network (ICN) Selection and Post processing—

After preprocessing the data, functional data from both control and patient groups were analyzed using spatial group independent component analysis (GICA) framework as implemented in the GIFT software (Calhoun and Adali, 2012; Calhoun et al., 2001; Erhardt et al., 2011). Spatial ICA decomposes the subject data into linear mixtures of spatially independent components that exhibit a unique time course profile. A subject-specific data reduction step was first used to reduce 162 time point data into 120 direction of maximal variability using principal component analysis. Then subject-reduced data were concatenated across time and a group data PCA step reduced this matrix further into 100 components along directions of maximal group variability. Note that, group PCA on the entire dataset was performed to avoid biasing the solution to group differences (Erhardt et al., 2011). One hundred independent components were obtained from the group PCA reduced matrix using the infomax algorithm (Bell and Sejnowski, 1995). To ensure stability of estimation, we repeated the ICA algorithm 20 times in ICASSO, and aggregate spatial maps were estimated as the modes of component clusters (Ma et al., 2011). Subject specific spatial maps (SMs) and time courses (TCs) were obtained using the spatiotemporal regression back reconstruction approach (Calhoun et al., 2001; Erhardt et al., 2011) implemented in the GIFT software.

Subject specific SMs and TCs underwent post-processing as described in our earlier work (Allen et al., 2012). Briefly, we obtained one sample t-test maps for each SM across all subjects and thresholded these maps to obtain regions of peak activation clusters for that component; we also computed mean power spectra of the corresponding TCs. We visually inspected and identified a set of components as intrinsic connectivity networks (ICNs) if their peak activation clusters fell on GM (gray matter) and showed less overlap with known vascular, susceptibility, ventricular, and edge regions corresponding to head motion. We also ensured that the mean power spectra of the selected ICN time courses showed higher low frequency spectral power. This selection procedure resulted in 47 ICNs out of the 100 independent components obtained. The ICNs were assessed and distributed into sub-cortical (SC), auditory (AUD), visual (VIS), sensorimotor (SM), attention/cognitive control (CC), default-mode (DMN), and cerebellar (CB) network domains.

Subject-specific TCs corresponding to the retained ICNs underwent additional post processing steps. The TCs were detrended to remove any existing linear, quadratic or cubic low frequency trends originating from scanner drift, orthogonalized with respect to estimated subject motion and realignment parameters, and despiked using AFNI's

Author Manuscript Author Manuscript Author Manuscript Author Manuscript

3dDespike function to replace outlier points with values estimated from third order spline fit to neighboring portions of the TCs.

2.3.3 FC Estimation and Clustering—Similar to our previous work (Damaraju et al., 2014) time-varying FNC was estimated by sliding a window of length 22 TRs (44 s) in steps of 1 TR (2 s). This sliding window analysis used a tapered window generated by convolving a rectangular window of length 22 TRs (44 s) with a Gaussian window of standard deviation equal to 3 TRs. To characterize the full covariance matrix, we estimated covariance from the regularized precision matrix or the inverse covariance matrix (Smith et al., 2011). Following the graphical LASSO method (Friedman et al., 2008), we placed a penalty on the L1 norm of the precision matrix to promote sparsity. The regularization parameter lambda was optimized separately for each subject by evaluating the log-likelihood of unseen data (windowed covariance matrices from the same subject) in a cross-validation framework. Final dynamic FC estimates for each window, were concatenated to form a C x C x W array representing the changes in covariance (correlation) between components as a function of time.

Next, we selected windows of higher variability as subject exemplars and used K-means clustering to obtain group centroids. We determined the number of clusters to be five using the elbow criterion of the cluster validity index, which is computed as the ratio between within-cluster distances to between-cluster distance. These centroids are then used as starting points to cluster all of the dynamic FNC data. Group- and subject- specific centroids were computed for further analyses (Allen et al., 2014).

2.4 Proposed pICA framework

Figure 1 and Figure S5 provides an illustration of the proposed framework. pICA was performed through the Fusion ICA Toolbox (FIT, http://mialab.mrn.org/software/fit) using the imaging (dynamic states) and genomic (SNP array) features. The algorithm was configured with a threshold of 0.25 for constrained correlations to avoid false positive associations and to only constrain one pair of components (Liu et al., 2009). A SNP component is defined by large clusters of functionally related SNPs statistically correlated with phenotype components, whereas a dFNC component is defined by clusters of related connectivity links among distant brain regions distributed across 5 discrete dynamic states, and statistically correlated with genomic components (Table S2). An endurance parameter was set to -5×10^{-4} to control the decreasing slope of the entropy term and to mitigate against over fitting. For the fMRI modality (dFNC features), the component number was predefined as 15, and for genomic modality (SNP data) the component number was predefined as 25 based on pICA model stability, which was validated using the permutation test. The parallel ICA estimates components by maximizing component independence within each data modality, and maximizing the inter-modality association assessed based on component loadings from the two modalities. In the current work, parallel ICA extracted 15 dFNC components and 25 SNP components, which led to a total of 375 SNP-dFNC pairs for which the associations were assessed. Significant SNP-dFNC associations were then identified based on Bonferroni correction ($p < 0.05/375$).

Author Manuscript Author Manuscript Author Manuscript Author Manuscript

We performed a 1000-run permutation test to assess the validity and stability of identified dFNC-SNP association by investigating the occurrences of inter-modality correlations by chance in permuted dFNC and SNP datasets (Chen et al., 2012). The null distribution was constructed with the top correlation obtained from each test run. We then counted the instances with correlations greater than that observed from the original data and calculated the two-tail probability as the significance level.

2.5 Polygenic Risk Score Analysis

Additionally, we computed the polygenic risk score (PRS) for SZ of the set of thresholded SNPs (i.e., top SNPs after thresholding the SNP component), which was a linearly weighted sum of the genotype profiles with weights derived from the odds ratios of the PGC SZ GWAS (Purcell, 2009; Ripke et al., 2014). The loading parameters from significant pICA paired components were then assessed for associations with PRS for SZ using Pearson's and Spearmann's rank order correlations.

2.6 Partial Replication Study

While an independent dataset with exact imaging and genomic features was unavailable for replication purpose, we implemented our proposed model on a separate, independent dataset for partial replication. The resting-state fMRI data were collected while the participants had their eyes open (as opposed to our main analyses where resting-state fMRI data were collected in eyes closed condition). We used resting-state functional magnetic resonance imaging (fMRI) data and single nucleotide polymorphism (SNP) data obtained from a local COBRE (center of biomedical research excellence) study. After preprocessing, we obtained data from a total of 135 participants (72 healthy controls and 63 SZ patients matched for age) for which both fMRI and SNP data were collected.

Using the same steps mentioned for our main analyses, we preprocessed both fMRI and SNP data. As the genomic features, we identified the same 1546 pre-selected SNPs as our main analyses. In order to identify the similar imaging features (i.e., dFNC states), we implemented the following two-step replication: (i) using a spatially constrained ICA approach, we computed subject specific maps and timecourses for the 49 ICNs and computed the sliding-window based dynamic connectivity matrices for each subject, and (ii) using k-means clustering approach while using the original dFNC states (i.e., from our main study) as stating points for clusters, we identified 5 cluster centroids/dFNC states for each subject. These dFNC states were then used as the imaging features for our proposed pICA framework.

The proposed algorithm proceeds in two stages, consisting of independent component computation at group and subject levels, respectively. First, a group-level ICA is performed to extract information in the form of group ICs from preprocessed fMRI data of multiple subjects. Then the group information is used as guidance for the subject-level ICA, computed separately on the fMRI data of each subject (Du and Fan, 2013; Du et al., 2015; Lin et al., 2010).

A list of key acronyms and definitions can be found in Tables S1 and S2.

Author Manuscript Author Manuscript Author Manuscript Author Manuscript

3 RESULTS

Figure 2 demonstrates the dFNC states for HC and SZ participants. The pICA framework identified one dFNC-SNP component pair with (i) significant correlation between the functional and genetic components, (ii) significant group difference in the functional component loading scores, and (iii) significant correlations between polygenic risk scores (PRS) and functional and genetic components. Figure 3 and Figure S3 show the significant component pair, with the connectivity strengths for the parallel co-varying functional component's inter-regional links or connections and Manhattan plot showing the SNP component. In order to display the top 5% of the connectivity links and SNPs, only links with connectivity strengths and SNPs with genomic component weights higher or lower than a cutoff value are shown. In particular, after converting to z-scores the genomic (SNP) component is thresholded at $|z|>2$ to retain only the top 5% SNPs, whereas the inter-regional connectivity strengths from the functional component, are thresholded at $|z|>3$ to retain only the top 5% connectivity links. For both functional and genetic components, we will hereafter refer to the retained inter-regional connections and top SNPs as "top links" and "top SNPs", respectively.

3.1 Parallel Significant Component

As illustrated in Figure 3 and Figure S3, the number of significant connections in the linked functional component were high for the temporal, parietal, limbic and occipital regions in state 1, whereas state 5 only had two significant connections, and **state 2, 3** and **4** had none. The peak activation coordinates of the significant links identified in **state 1** and **state 5** are presented in Table 4. In terms of occupancy rate, state 1 was dominated by the healthy subjects (HC=22%; SZ=14%), whereas state 5 was dominated by schizophrenia patients (HC=16%; SZ=27%). Note that, a positive connectivity is defined as the positive correlation strength between two brain networks (ICNs), and depicted with red color within the connectogram plots (i.e., the greater the positive connectivity strength is, the darker red color is used as per the color bar), whereas a negative connectivity is defined as the negative or anti-correlation strength between two brain networks (ICNs), and depicted with blue color within the connectogram plots (i.e., the greater the negative connectivity strength is, the darker blue color is used as per the color bar)

The significant SNP component was first z-scored and then absolute z-scored values were used to represent the normalized component weight. The SNP component consists of peak weights of SNPs mostly located in chromosome 6 (and few at chromosomes 1, 2, 3,5, 15 and 17). The significant SNP component was predominantly contributed to by 80 SNPs (Table 5; top 5% based on absolute values of the component weights). 24 SNPs were mapped to 13 unique genes using UCSC hg19 assembly (http://hgdownload.cse.ucsc.edu/), while the rest were from inter-genic regions.

The correlation between the significant (i.e., after the correlations identified by pICA which were controlled for diagnosis were corrected for multiple comparisons), parallel co-varying dFNC and SNP components was: Pearson's $r= 0.5223$ ($p< 6.95 \times 10\text{-}9$) and Spearmann's: $r = 0.4952$ ($p < 6.95 \times 10\text{-}9$). In a 1000-run permutation test, the absolute values of the dFNC-

Author Manuscript Author Manuscript Author Manuscript Author Manuscript

SNP top correlations ranged from 0.15 to 0.67 with a median of 0.26, yielding a p-value of 1.1×10^{-2}.

3.2 Group Differences in Component Loadings

Figure 4a presents the scatterplot of the significant parallel components' loading parameters, with a pattern of positively increasing relationship between these two loading parameters. Figures 4b and 4c show the group-wise loading parameters in healthy control and schizophrenia populations estimated from dFNC and SNP components, respectively. The ANOVA showed a significant group difference in the dFNC loading parameter (p=0.008), with a lower dFNC mean loading in the SZ group (mean=0.0066, standard deviation=0.0159) compared to the control group (mean=0.0152, standard deviation=0.0212). There was no significant group difference in the SNP loading parameter (p=0.243), although the group mean SNP loading was lower in the SZ group (mean= −0.0265, standard deviation=0.0977) compared to the healthy group (mean=- 0.0069, standard deviation=0.1012). This validates our pICA approach as typically between group effect sizes for imaging data are much larger than those for genomic data.

3.3 Risk Score and Component Loadings

We also assessed the correlations between the polygenic risk scores (PRS) and both dFNC and SNP components' loading parameters. The PRS was computed from the top SNPs (i.e., 80 SNPs after thresholding the SNP component at |z|>2)) of the linked SNP component. The PRS computed using the top SNPs ranged between 0 and −8. The scatterplots of PRS versus component loadings are shown in Figure 5. The correlation between the risk scores and dFNC loadings was: Pearson's r= −0.26 (p=0.0017); Spearmann's r=−0.2743 (p=7.7230e-4), whereas the correlation between the risk scores and SNP loadings was: Pearson's r= −0.5401 (p=1.4×10-12); Spearmann's r=−0.5406 (p =< 6.95 × 10-9). Results show that, as the risk of SZ increases, the loading coefficients associated with the dFNC component decrease, suggesting that the SZ patients tend to under-utilize the vast amount of connections available through the brain regions, particularly SZ patients have the poor utilization of the top links in state 1 (mostly among temporal, parietal, limbic and occipital regions, see Figure S3 and Table 4 for more details). Interestingly, the SZ group showed low occupancy rate in state 1 compared to the HC group (HC=22%; SZ=14%) suggesting lower occupancy of that state may be a marker of schizophrenia risk.

3.4 Pathway Analysis Using Top Genes

We examined the genetic architecture of our findings using Reactome Pathway Analysis (RPA: https://www.reactome.org), where the 13 genes were compared with the preselected SNPs as background. The results obtained from RPA are provided in Table 2. Further, GeneMANIA (Mostafavi et al., 2008) was used to identified the interactions among the query genes. We also analyzed our query genes to find the biological functions of these top genes, which are provided in Table 3.

Author Manuscript Author Manuscript Author Manuscript Author Manuscript

3.5 Parallel Significant Component From Partial Replication Study

The results from pICA framework captured a significant imaging (dFNC) and genomic (SNPs) component pair with a correlation of r= 0.22 (p=0.0099). The correlation between the main (fBIRN) and replication dataset () SNPs components was 0.28 (p<0.0005). However, the correlation between dFNC components was not significant (r= 0.01,p=0.46). We speculate that, due to different imaging data acquisition conditions (eyes closed versus eyes open) (Wu et al., 2010), we were unable to replicate the imaging part of the pICA component. Future work should implement replication using an independent dataset with similar features in order to systematically verify our findings from this pilot study.

In summary, here we have investigated the genomic underpinnings of dysfunctional dynamic FNC in SZ. A multivariate approach, pICA, was used to extract SNP and dFNC components, and retrieve intermodality associations. We investigated the relationship between genomic data and time-varying FNC measures and explored characteristic brain abnormalities with regard to schizophrenia. By employing a novel approach, we first estimated relatively lower-dimensional feature spaces from the high-dimensional fMRI and SNP array data. Next, we performed a multivariate data fusion approach on these estimated lower-dimensional feature spaces by implementing a pICA approach to extract corresponding co-varying genetic and functional brain components and evaluated associations between the components. Due to the limited sample size compared to genome-wide SNPs, we preselected 1546 SZ risk loci based upon large-scale GWAS in the published PGC study (Ripke et al., 2014) to focus the dFNC-SNP association analysis on polymorphisms likely relevant to SZ. One significant dFNC-SNP pair was identified and the permutation test indicated a low possibility that the observed correlation was due to overfitting, though the current result still awaits further independent validation.

4. DISCUSSION

In this study, we have investigated the relationship between neuroimaging and genomic features in patients with SZ. In particular, our results captured one pICA component pair that exhibited significant correlation between their underlying modality-specific components, highlighting significant group differences in time-varying FNC component loadings, and significant negative correlations between polygenic risk scores (PRSs) and both dFNC and SNP component. The pICA dFNC and SNP components showed a significant positive correlation of r=0.5223 ($p<6.95e^{-09}$), as depicted in Figure 4a. This implies that, individuals that load more heavily on the top SNPs (and therefore the unique genes that these SNPs are map into) show more increased (or more decreased) functional connectivity among brain networks that underlie the functional component capturing top positive (and negative) connectivity strengths (i.e., top links in **state 1** and **5**).

Substantial correspondence with previously reported studies in literature could also be drawn for few evaluated top inter-regional (i.e., inter-ICN) links in the estimated functional components. First, the functional component for the retained parallel source showed top connectivity links in time-varying connectivity **states 1** and **5**. Most of the top inter-ICN links are captured in **state 1**, a state more often occupied by healthy individuals, where both positive and negative connectivity strengths across various network domains can be observed

Author Manuscript Author Manuscript Author Manuscript Author Manuscript

(Figure 3). In particular, a CC domain component, IC47 (cingulate gyrus), showed inter-ICN link with components from several domains including VIS (IC60: right precuneus/left cuneus; IC78: right cuneus and IC 80: middle temporal gyrus), SM (IC63: fusiform gyrus; IC6: right postcentral gyrus and IC10: left precentral gyrus) and DMN (IC53: left anterior cingulate gyrus; IC69: right medial frontal gyrus; IC84: right angular gyrus and IC90: right angular gyrus). Additionally, in this state, ICNs in the DMN domain showed connectivity within themselves and with ICNs from CC and VIS domains as well. For example, one of the DMN ICNs, IC84, highlighted by the brain regions in right angular gyrus (parietal component), showed positive connectivity weight with an ICN from the VIS domain characterized by calcarine gyrus (IC91, occipital component) and negative connectivity weight with a CC ICN, cingulate gyrus (IC47, limbic component). Another DMN ICN, IC90, encompassing the right angular gyrus also showed negative connectivity weights with two ICNs from the VIS and CC domains, right calcarine gyrus (IC43, occipital component) and cingulate gyrus (IC47, limbic component). Moreover, two DMN ICNs, IC53 (left anterior cingulate gyrus, limbic component) and IC95 (left angular gyrus, parietal component) have shown positive connectivity weight between themselves. These results are in line with a previous reports that have shown aberrant connectivity patterns within regions including angular gyrus, calcarine gyrus and cingulate sub-regions in schizophrenia patients (Rashid et al., 2014; Wang et al., 2015). Indeed, the roles of angular gyrus in language processing, memory and social cognition have been extensively reported (Binder et al., 2009; Clos et al., 2014; Hall et al., 2005). Disrupted DMN connectivity in schizophrenia patients has been extensively reported by several recent studies (Garrity et al., 2007; Ongur et al., 2010; Rashid et al., 2014). Thus, further follow-up examination of these top links involving the DMN ICNs is warranted. Interestingly, four temporal lobe components, IC63 (fusiform gyrus), IC80 (middle temporal gyrus), IC51 (middle temporal gyrus) and IC57 (parahippocampal gyrus) showed connectivity with limbic (IC47: cingulate gyrus), frontal (IC5: precentral gyrus) and occipital (IC7: right cuneus) components. Previous studies have reported disrupted temporal lobe connectivity in schizophrenia (Alonso-Solis et al., 2015; Barta et al., 1990; £etin et al., 2014; Ford et al., 2002; Peters et al., 2016; Wolf et al., 2007), suggesting that components within the temporal lobe play an important role in schizophrenia disease etiology. However, further investigation is required to validate the role of temporal lobe dysfunction in schizophrenia with regard to the current imaging-genomics framework.

Dynamic connectivity **state 1** also captured a CC ICN, left precuneus (IC35, parietal component) showing negative connectivity weight with a VIS component, right lingual gyrus (IC91, occipital component). Patterns of disrupted connectivity in schizophrenia within the precuneus and lingual gyrus have been reported (Kühn and Gallinat, 2011; Rashid et al., 2014; Zhu et al., 2017). Precuneus is involved in episodic memory (Rugg and Henson, 2002), mental imagery recall (Fletcher et al., 1996), and self-processing operations (Cavanna and Trimble, 2006), whereas lingual gyrus is involved in visual processing (Bogousslavsky et al., 1987). In **state 2**, positive connectivity weight between two VIS domain ICNs, right cuneus (IC7, occipital component) and right calcarine gyrus (IC43, occipital component), and negative connectivity weight between a CC domain ICN, cingulate gyrus (IC47, limbic component) and a SM domain component, precentral gyrus (IC5, frontal component) have been observed. While we evaluate only a few interesting links within the scope of the current

Author Manuscript Author Manuscript Author Manuscript Author Manuscript

work, there is much more that could be done to explore these results to further expand our understanding of the genomic- connectivity relationships and further contribute to characterization of schizophrenia.

While inter-modality association is assessed based on loading vectors, interpretation of source of variance is based on component scores. Figure S3(a) demonstrates the top connectivity features obtained with thresholding the dFNC component scores at $|z| > 3$. In the ICA framework, the corresponding loading vector largely captures the covariation of these top features. Figure S3(b) shows that these top features majorly comprise regional connectivities of State-1 and State-5, involving mostly brain regions of temporal, parietal, limbic and occipital areas (see Table 4 for details on the top brain regions). In parallel, the SNP loading vector primarily reflects the covariation among the 80 top SNPs obtained with thresholding the SNP component scores at $|z| > 2$, as shown in Figure S3(c). Collectively, the identified SNP-dFNC association indicates that the across-subject covariation pattern of the top 80 SNPs explains 11.55% of the variance in the across- subject covariation pattern of the top connectivity feature (i.e., top links). Our results imply that the identified 13 genes mapped from the thresholded 80 SNPs derived from the significant pICA component (for details on the derivation steps of these thresholded SNPs and the mapped genes, see Figure S5) might mediate the dysfunctional connectivity links (observed among the thresholded dFNC component's connectivity links found in State-1 and State-5, Figure S3) among these brain regions in patients with SZ.

The identified pICA component revealed significant group differences in dFNC loading parameters, where patients with SZ exhibited a significantly lower group mean compared to the HC group. This could imply that, for the significant links within dFNC component, SZ individuals have diminished capability to establish links between these brain regions and share information. We also assessed the correlations between the polygenic risk scores (PRS) and both dFNC and SNP components' loading parameters. Also, the correlations between the polygenic risk scores (PRS) and dFNC loadings were significantly negative (Figure 5). For dFNC component, thresholded top links were observed mostly in state 1, a state that is dominated by the healthy controls in terms of occupancy rate (Table 1; HC=22% and SZ=14%). This could imply that, as the polygenic risk scores increase for individuals (as measured using PRS), chances to load onto the links within **state 1** decrease.

Using GeneMANIA (Mostafavi et al., 2008) we estimated the percentages of co expression and genetic interaction among the 13 query genes (where co-expression measures whether the genes have similar expression levels across conditions and therefore are linked, and genetic interaction assesses whether the genes are functionally associated by identifying if perturbing one gene would result in perturbations to a second gene). The result obtained from GeneMANIA shows that 40.49 % of the 13 listed genes show co-expression. There is 59.51% genetic interaction among the query genes. A Reactome Pathway Analysis (RPA) (Croft et al., 2013) further shows that these selected genes are involved in different cellular processes including the immune system, metabolism and neuronal systems (Table 2). Among the top 13 genes, *CHRNA3, ATXN7* and *SMG6* are found to be involved in neurological, psychological and developmental disorders, while *RERE* and *HLA-C* are involved in immunological disease (Table 3). Indeed, previous evidence indicated that

Author Manuscript Author Manuscript Author Manuscript Author Manuscript

sensorimotor gating is influenced by variations of the *CHRNA3* gene, and might affect the course and severity of schizophrenia (Petrovsky et al., 2010). Moreover, a recent pICA based work explored the genetic control over the DMN in SZ and psychotic bipolar disorder patients, and identified the underlying biological pathways and neurodevelopment/transmission processes including PKA, immune response signaling, NMDA-related long-term potentiation, axon guidance, and synaptogenesis that significantly influenced DMN disconnectivity (Meda et al., 2014). Taken together, the proposed pICA framework presents a powerful way to understand how disrupted connectivity in SZ can be mediated by underlying genes, which could lead us to potential disease-specific biomarkers.

6. LIMITATION AND FUTURE DIRECTION

This is the first study to examine the link between genetic data and resting-state dynamic functional connectivity in schizophrenia and healthy controls using a simultaneous ICA (pICA) approach. The samples in this study, although albeit small, were well characterized, and the pICA approach is a powerful method to examine dFNC-SNP relationships. While the current findings unravel few important aspects of the proposed model, there were some limitations. First, sample sizes in this study were small, so future studies should endeavor to replicate these findings in larger samples. Second, for our replication study, one dataset acquired fMRI data while participants were resting with their eyes closed (fBIRN), and the other dataset acquired fMRI data while participants were resting with their eyes open (COBRE). Recent studies investigating dynamic FNC found difference in patterns of connectivity measure between eyes open and eyes condition (Allen et al., 2018). While we have partially replicated our pICA findings, future studies should investigate independent dataset with same acquisition paradigms (i.e., eyes closed) for full replication. Finally, based on the known dynamic nature of the brain and the unconstrained nature of resting fMRI data, we utilized dFNC as our imaging modality-related features. As a future investigation, an extension of this work should compare performance of the proposed pICA framework using sFNC versus dFNC features. The dFNC-SNP association presented here is the first step showing the strength of the proposed framework, and future work will involve investigation of other potential connectivity references, for association with genomic data.

7. CONCLUSION

In summary, using a multivariate pICA based fusion approach, we propose a framework to identify and investigate parallel co-varying SNP and dFNC components that might uncover genetic contributions to disrupted dynamic connectivity in schizophrenia. We demonstrate that studying such interactions can provide a powerful way of evaluating gene-brain relationships to characterizing schizophrenia and other mental illnesses.

Supplementary Material

Refer to Web version on PubMed Central for supplementary material.

Acknowledgments

FUNDING

Author Manuscript Author Manuscript Author Manuscript Author Manuscript

This work was supported by the National Institutes of Health (NIH) grants (P20GM103 472/5P20RR021938, R01EB005846, 1R01EB006841, R01REB020407, R01EB000840) and the National Science Foundation (NSF) grant #1539067.

References

Abrol A, Chaze C, Damaraju E, Calhoun VD, 2016 The chronnectome: Evaluating replicability of dynamic connectivity patterns in 7500 resting fMRI datasets. Engineering in Medicine and Biology Society (EMBC), 2016 IEEE 38th Annual International Conference of the. IEEE, pp. 5571–5574.

Abrol A, Damaraju E, Miller RL, Stephen JM, Claus ED, Mayer AR, Calhoun VD, 2017 Replicability of time-varying connectivity patterns in large resting state fMRI samples. Neuroimage 163, 160–176. [PubMed: 28916181]

Allen E, Damaraju E, Eichele T, Wu L, Calhoun V, 2018 EEG signatures of dynamic functional network connectivity states. Brain topography 31, 101–116. [PubMed: 28229308]

Allen EA, Damaraju E, Plis SM, Erhardt EB, Eichele T, Calhoun VD, 2014 Tracking whole-brain connectivity dynamics in the resting state. Cerebral cortex 24, 663–676. [PubMed: 23146964]

Alonso-Solís A, Vives-Gilabert Y, Grasa E, Portella MJ, Rabella M, Sauras RB, … Pérez V, 2015 Resting-state functional connectivity alterations in the default network of schizophrenia patients with persistent auditory verbal hallucinations. Schizophrenia research 161, 261–268. [PubMed: 25468173]

Altshuler DM, Durbin RM, Abecasis GR, Bentley DR, Chakravarti A, Clark AG,… Consortium GP, 2012 An integrated map of genetic variation from 1,092 human genomes. Nature 491, 56–65. [PubMed: 23128226]

Barta PE, Pearlson GD, Powers RE, Richards SS, Tune LE, 1990 Auditory hallucinations and smaller superior temporal gyral volume in schizophrenia. The American journal of psychiatry 147, 1457. [PubMed: 2221156]

Bassett DS, Nelson BG, Mueller BA, Camchong J, Lim KO, 2012 Altered resting state complexity in schizophrenia. Neuroimage 59, 2196–2207. [PubMed: 22008374]

Bell AJ, Sejnowski TJ, 1995 An information-maximization approach to blind separation and blind deconvolution. Neural computation 7, 1129–1159. [PubMed: 7584893]

Binder JR, Desai RH, Graves WW, Conant LL, 2009 Where is the semantic system? A critical review and meta-analysis of 120 functional neuroimaging studies. Cerebral cortex 19, 2767–2796. [PubMed: 19329570]

Bogousslavsky J, Miklossy J, Deruaz J-P, Assal G, Regli F, 1987 Lingual and fusiform gyri in visual processing: a clinico-pathologic study of superior altitudinal hemianopia. Journal of Neurology, Neurosurgery & Psychiatry 50, 607–614.

Calhoun V, Adali T, Giuliani N, Pekar J, Kiehl K, Pearlson G, 2006 Method for multimodal analysis of independent source differences in schizophrenia: combining gray matter structural and auditory oddball functional data. Human brain mapping 27, 47–62. [PubMed: 16108017]

Calhoun VD, Adali T, 2012 Multisubject independent component analysis of fMRI: a decade of intrinsic networks, default mode, and neurodiagnostic discovery. IEEE reviews in biomedical engineering 5, 60–73. [PubMed: 23231989]

Calhoun VD, Adali T, Pearlson GD, Pekar J, 2001 A method for making group inferences from functional MRI data using independent component analysis. Human brain mapping 14, 140–151. [PubMed: 11559959]

Calhoun VD, Miller R, Pearlson G, Adali T, 2014 The chronnectome: time- varying connectivity networks as the next frontier in fMRI data discovery. Neuron 84, 262–274. [PubMed: 25374354]

Calhoun VD, Sui J, 2016 Multimodal fusion of brain imaging data: A key to finding the missing link (s) in complex mental illness. Biological psychiatry: cognitive neuroscience and neuroimaging 1, 230–244. [PubMed: 27347565]

Calhoun VD, Sui J, Kiehl K, Turner JA, Allen EA, Pearlson G, 2012 Exploring the psychosis functional connectome: aberrant intrinsic networks in schizophrenia and bipolar disorder. Frontiers in psychiatry 2, 75. [PubMed: 22291663]

Author Manuscript Author Manuscript Author Manuscript Author Manuscript

Calhoun VD, Wager TD, Krishnan A, Rosch KS, Seymour KE, Nebel MB, …Kiehl K, 2017 The impact of T1 versus EPI spatial normalization templates for fMRI data analyses. Human brain mapping 38, 5331–5342. [PubMed: 28745021]

Cardno AG, Gottesman II, 2000 Twin studies of schizophrenia: from bow - and - arrow concordances to star wars Mx and functional genomics. American Journal of Medical Genetics Part A 97, 12–17.

Cavanna AE, Trimble MR, 2006 The precuneus: a review of its functional anatomy and behavioural correlates. Brain 129, 564–583. [PubMed: 16399806]

Çetin MS, Christensen F, Abbott CC, Stephen JM, Mayer AR, Canive JM, …Calhoun VD, 2014 Thalamus and posterior temporal lobe show greater internetwork connectivity at rest and across sensory paradigms in schizophrenia. Neuroimage 97, 117–126. [PubMed: 24736181]

Chen J, Calhoun VD, Lin D, Perrone-Bizzozero NI, Bustillo JR, Pearlson GD, … Ehrlich S, 2018 Shared Genetic Risk of Schizophrenia and Gray Matter Reduction in 6p22. 1. Schizophrenia bulletin Epub.

2012 Multifaceted genomic risk for brain function in schizophrenia. Neuroimage 61, 866–875. [PubMed: 22440650]

Chen J, Calhoun VD, Pearlson GD, Perrone-Bizzozero N, Sui J, Turner JA, …Cañive JM, 2013 Guided exploration of genomic risk for gray matter abnormalities in schizophrenia using parallel independent component analysis with reference. Neuroimage 83, 384–396. [PubMed: 23727316]

Chen K, Reiman EM, Huan Z, Caselli RJ, Bandy D, Ayutyanont N, Alexander GE, 2009 Linking functional and structural brain images with multivariate network analyses: a novel application of the partial least square method. Neuroimage 47, 602–610. [PubMed: 19393744]

Clos M, Langner R, Meyer M, Oechslin MS, Zilles K, Eickhoff SB, 2014 Effects of prior information on decoding degraded speech: an fMRI study. Human brain mapping 35, 61–74. [PubMed: 22936472]

Correa N, Adali T, Calhoun VD, 2007 Performance of blind source separation algorithms for fMRI analysis using a group ICA method. Magnetic resonance imaging 25, 684–694. [PubMed: 17540281]

Croft D, Mundo AF, Haw R, Milacic M, Weiser J, Wu G, …Kamdar MR, 2013 The Reactome pathway knowledgebase. Nucleic acids research 42, D472–D477. [PubMed: 24243840]

Damaraju E, Allen EA, Belger A, Ford J, McEwen S, Mathalon D, …Preda, A., 2014 Dynamic functional connectivity analysis reveals transient states of dysconnectivity in schizophrenia. Neuroimage: Clinical 5, 298–308.

Delaneau O, Marchini J, Zagury JF, 2011 A linear complexity phasing method for thousands of genomes. Nat Methods 9, 179–181. [PubMed: 22138821]

Du Y, Fan Y, 2013 Group information guided ICA for fMRI data analysis. Neuroimage 69, 157–197. [PubMed: 23194820]

Du Y, Pearlson GD, Liu J, Sui J, Yu Q, He H, …Calhoun VD, 2015 A group ICA based framework for evaluating resting fMRI markers when disease categories are unclear: application to schizophrenia, bipolar, and schizoaffective disorders. Neuroimage 122, 272–280. [PubMed: 26216278]

Elliott L, Sharp K, Alfaro-Almagro F, Douaud G, Miller K, Marchini J, Smith S, 2017 The genetic basis of human brain structure and function: 1,262 genome-wide associations found from 3,144 GWAS of multimodal brain imaging phenotypes from 9,707 UK Biobank participants. BioRxiv, 178806.

Ellison-Wright I, Bullmore E, 2010 Anatomy of bipolar disorder and schizophrenia: a meta-analysis. Schizophrenia research 117, 1–12. [PubMed: 20071149]

Erhardt EB, Rachakonda S, Bedrick EJ, Allen EA, Adali T, Calhoun VD, 2011 Comparison of multi - subject ICA methods for analysis of fMRI data. Human brain mapping 32, 2075–2095. [PubMed: 21162045]

Fletcher P, Shallice T, Frith C, Frackowiak R, Dolan R, 1996 Brain activity during memory retrieval: The influence of imagery and semantic cueing. Brain 119, 1587–1596. [PubMed: 8931582]

Ford JM, Mathalon DH, Whitfield S, Faustman WO, Roth WT, 2002 Reduced communication between frontal and temporal lobes during talking in schizophrenia. Biological psychiatry 51, 485–492. [PubMed: 11922884]

Author Manuscript Author Manuscript Author Manuscript Author Manuscript

Freire L, Mangin J-F, 2001 Motion correction algorithms may create spurious brain activations in the absence of subject motion. Neuroimage 14, 709–722. [PubMed: 11506543]

Friedman J, Hastie T, Tibshirani R, 2008 Sparse inverse covariance estimation with the graphical lasso. Biostatistics 9, 432–441. [PubMed: 18079126]

Friedman L, Glover GH, Krenz D, Magnotta V, 2006 Reducing inter-scanner variability of activation in a multicenter fMRI study: role of smoothness equalization. Neuroimage 32, 1656–1668. [PubMed: 16875843]

Fu Y, Ma Z, Hamilton C, Liang Z, Hou X, Ma X, …Wang Y, 2015 Genetic influences on resting - state functional networks: A twin study. Human brain mapping 36, 3959–3972. [PubMed: 26147340]

Garrity AG, Pearlson GD, McKiernan K, Lloyd D, Kiehl KA, Calhoun VD, 2007 Aberrant "default mode" functional connectivity in schizophrenia. American Journal of Psychiatry 164, 450–457. [PubMed: 17329470]

Glahn DC, Winkler A, Kochunov P, Almasy L, Duggirala R, Carless M, …Smith S, 2010 Genetic control over the resting brain. Proceedings of the National Academy of Sciences 107, 1223–1228.

Gottesman II, Gould TD, 2003 The endophenotype concept in psychiatry: etymology and strategic intentions. American Journal of Psychiatry 160, 636–645. [PubMed: 12668349]

Gottesman II, Shields J, 1972 A polygenic theory of schizophrenia. International Journal of Mental Health 1, 107–115.

Groves AR, Beckmann CF, Smith SM, Woolrich MW, 2011 Linked independent component analysis for multimodal data fusion. Neuroimage 54, 2198–2217. [PubMed: 20932919]

Gupta CN, Calhoun VD, Rachakonda S, Chen J, Patel V, Liu J, …Arias-Vasquez A, 2014 Patterns of gray matter abnormalities in schizophrenia based on an international mega-analysis. Schizophrenia bulletin 41, 1133–1142. [PubMed: 25548384]

Hall DA, Fussell C, Summerfield AQ, 2005 Reading fluent speech from talking faces: typical brain networks and individual differences. Journal of Cognitive Neuroscience 17, 939–953. [PubMed: 15969911]

Harris GJ, Chabris CF, Clark J, Urban T, Aharon I, Steele S, …Tager-Flusberg G, 2006 Brain activation during semantic processing in autism spectrum disorders via functional magnetic resonance imaging. Brain and cognition 61, 54–68. [PubMed: 16473449]

Hindorff LA, Sethupathy P, Junkins HA, Ramos EM, Mehta JP, Collins FS, Manolio TA, 2009 Potential etiologic and functional implications of genome-wide association loci for human diseases and traits. Proceedings of the National Academy of Sciences 106, 9362–9367.

Hirschhorn JN, Daly MJ, 2005 Genome-wide association studies for common diseases and complex traits. Nature Reviews Genetics 6, 95.

Hutchison RM, Womelsdorf T, Allen EA, Bandettini PA, Calhoun VD, Corbetta M, … Gonzalez-Castillo J, 2013 Dynamic functional connectivity: promise, issues, and interpretations. Neuroimage 80, 360–378. [PubMed: 23707587]

Ivleva EI, Bidesi AS, Thomas BP, Meda SA, Francis A, Moates AF, … Tamminga CA, 2012 Brain gray matter phenotypes across the psychosis dimension. Psychiatry Research: Neuroimaging 204, 13–24. [PubMed: 23177922]

Jafri MJ, Pearlson GD, Stevens M, Calhoun VD, 2008 A method for functional network connectivity among spatially independent resting-state components in schizophrenia. Neuroimage 39, 1666–1681. [PubMed: 18082428]

Jagannathan K, Calhoun VD, Gelernter J, Stevens MC, Liu J, Bolognani F, … Pearlson GD, 2010 Genetic associations of brain structural networks in schizophrenia: a preliminary study. Biological psychiatry 68, 657–666. [PubMed: 20691427]

Kendler K, Eaves L, 2005 Psychiatric genetics (review of psychiatry). Arlington, VA: American Psychiatric Publishing, Inc.

Keshavan MS, Morris DW, Sweeney JA, Pearlson G, Thaker G, Seidman LJ, … Tamminga C, 2011 A dimensional approach to the psychosis spectrum between bipolar disorder and schizophrenia: the Schizo-Bipolar Scale. Schizophrenia research 133, 250–254. [PubMed: 21996268]

Koyama MS, Kelly C, Shehzad Z, Penesetti D, Castellanos FX, Milham MP, 2010 Reading networks at rest. Cerebral cortex 20, 2549–2559. [PubMed: 20139150]

Author Manuscript Author Manuscript Author Manuscript Author Manuscript

Kühn S, Gallinat J, 2011 Resting-state brain activity in schizophrenia and major depression: a quantitative meta-analysis. Schizophrenia bulletin 39, 358–365. [PubMed: 22080493]

Lichtenstein P, Yip BH, Björk C, Pawitan Y, Cannon TD, Sullivan PF, Hultman CM, 2009 Common genetic determinants of schizophrenia and bipolar disorder in Swedish families: a population-based study. The Lancet 373, 234–239.

Lin QH, Liu J, Zheng YR, Liang H, Calhoun VD, 2010 Semiblind spatial ICA of fMRI using spatial constraints. Human brain mapping 31, 1076–1088. [PubMed: 20017117]

Liu J, Calhoun VD, 2014 A review of multivariate analyses in imaging genetics. Frontiers in neuroinformatics 8, 29. [PubMed: 24723883]

Liu J, Pearlson G, Windemuth A, Ruano G, Perrone - Bizzozero NI, Calhoun V, 2009 Combining fMRI and SNP data to investigate connections between brain function and genetics using parallel ICA. Human brain mapping 30, 241–255. [PubMed: 18072279]

Ma S, Correa NM, Li X-L, Eichele T, Calhoun VD, Adali T, 2011 Automatic identification of functional clusters in FMRI data using spatial dependence. IEEE Transactions on Biomedical Engineering 58, 3406–3417. [PubMed: 21900068]

Manoach DS, Gollub RL, Benson ES, Searl MM, Goff DC, Halpern E, … Rauch SL, 2000 Schizophrenic subjects show aberrant fMRI activation of dorsolateral prefrontal cortex and basal ganglia during working memory performance. Biological psychiatry 48, 99–109. [PubMed: 10903406]

Manoliu A, Riedl V, Doll A, Bauml JG, Muhlau M, Schwerthoffer D, … Bauml J,2012 Insular dysfunction reflects altered between-network connectivity and severity of negative symptoms in schizophrenia during psychotic remission. Frontiers in human neuroscience 7, 216.

Marchini J, Howie B, 2010 Genotype imputation for genome-wide association studies. Nat Rev Genet 11, 499–511. [PubMed: 20517342]

Meda SA, Gill A, Stevens MC, Lorenzoni RP, Glahn DC, Calhoun VD, … Thaker G, 2012 Differences in resting-state functional magnetic resonance imaging functional network connectivity between schizophrenia and psychotic bipolar probands and their unaffected first-degree relatives. Biological psychiatry 71, 881–889. [PubMed: 22401986]

Meda SA, Jagannathan K, Gelernter J, Calhoun VD, Liu J, Stevens MC, Pearlson GD, 2010 A pilot multivariate parallel ICA study to investigate differential linkage between neural networks and genetic profiles in schizophrenia. Neuroimage 53, 1007–1015. [PubMed: 19944766]

Meda SA, Ruano G, Windemuth A, O'Neil K, Berwise C, Dunn SM, … Sprooten E, 2014 Multivariate analysis reveals genetic associations of the resting default mode network in psychotic bipolar disorder and schizophrenia. Proceedings of the National Academy of Sciences 111, E2066–E2075.

Miller RL, Adali T, Levin-Schwartz Y, Calhoun VD, 2017 Resting-state fMRI dynamics and null models: perspectives, sampling variability, and simulations. BioRxiv, 153411.

Monks PJ, Thompson JM, Bullmore ET, Suckling J, Brammer MJ, Williams SC, … Louise Harrison C, 2004 A functional MRI study of working memory task in euthymic bipolar disorder: evidence for task - specific dysfunction. Bipolar Disorders 6, 550–564. [PubMed: 15541071]

Mostafavi S, Ray D, Warde-Farley D, Grouios C, Morris Q, 2008 GeneMANIA: a real-time multiple association network integration algorithm for predicting gene function. Genome biology 9, S4.

Ongur D, Lundy M, Greenhouse I, Shinn AK, Menon V, Cohen BM, Renshaw PF, 2010 Default mode network abnormalities in bipolar disorder and schizophrenia. Psychiatry Research: Neuroimaging 183, 59–68. [PubMed: 20553873]

Pearlson G, Calhoun VD, 2009 Convergent approaches for defining functional imaging endophenotypes in schizophrenia. Frontiers in human neuroscience 3, 37. [PubMed: 19956400]

Pearlson GD, Calhoun VD, Liu J, 2015 An introductory review of parallel independent component analysis (p-ICA) and a guide to applying p-ICA to genetic data and imaging phenotypes to identify disease-associated biological pathways and systems in common complex disorders. Frontiers in genetics 6, 276. [PubMed: 26442095]

Peters H, Shao J, Scherr M, Schwerthoffer D, Zimmer C, Forstl H, … Koch, K., 2016 More consistently altered connectivity patterns for cerebellum and medial temporal lobes than for amygdala and striatum in schizophrenia. Frontiers in human neuroscience 10, 55. [PubMed: 26924973]

Author Manuscript Author Manuscript Author Manuscript Author Manuscript

Petrella J, Sheldon F, Prince S, Calhoun V, Doraiswamy P, 2011 Default mode network connectivity in stable vs progressive mild cognitive impairment. Neurology 76, 511–517. [PubMed: 21228297]

Petrovsky N, Quednow BB, Ettinger U, Schmechtig A, Mossner R, Collier DA, … Kumari, V., 2010 Sensorimotor gating is associated with CHRNA3 polymorphisms in schizophrenia and healthy volunteers. Neuropsychopharmacology 35, 1429. [PubMed: 20393456]

Potkin SG, Ford JM, 2008 Widespread cortical dysfunction in schizophrenia: the FBIRN imaging consortium. Schizophrenia bulletin 35, 15–18. [PubMed: 19023124]

Preti MG, Bolton TA, Van De Ville D, 2017 The dynamic functional connectome: State-of-the-art and perspectives. Neuroimage 160, 41–54. [PubMed: 28034766]

Price AL, Patterson NJ, Plenge RM, Weinblatt ME, Shadick NA, Reich D, 2006 Principal components analysis corrects for stratification in genome-wide association studies. Nat Genet 38, 904–909. [PubMed: 16862161]

Purcell S, 2009 International Schizophrenia ConsortiumWray NR, Stone JL, Visscher PM, O'Donovan MC, Sullivan PF, Sklar P. Common polygenic variation contributes to risk of schizophrenia and bipolar disorder. Nature 460, 748–752. [PubMed: 19571811]

Purcell S, Neale B, Todd-Brown K, Thomas L, Ferreira MA, Bender D, … Daly MJ, 2007 PLINK: a tool set for whole-genome association and population-based linkage analyses. The American Journal of Human Genetics 81, 559–575. [PubMed: 17701901]

Rashid B, Arbabshirani MR, Damaraju E, Cetin MS, Miller R, Pearlson GD, Calhoun VD, 2016 Classification of schizophrenia and bipolar patients using static and dynamic resting-state fMRI brain connectivity. Neuroimage 134, 645–657. [PubMed: 27118088]

Rashid B, Damaraju E, Pearlson GD, Calhoun VD, 2014 Dynamic connectivity states estimated from resting fMRI Identify differences among Schizophrenia, bipolar disorder, and healthy control subjects. Frontiers in human neuroscience 8, 897. [PubMed: 25426048]

Ripke S, Neale BM, Corvin A, Walters JT, Farh K-H, Holmans PA, … Huang H,Biological insights from 108 schizophrenia-associated genetic loci. Nature 511, 421. [PubMed: 25056061]

Rugg MD, Henson RN, 2002 Episodic memory retrieval: an (event-related) functional neuroimaging perspective. The cognitive neuroscience of memory encoding and retrieval, 3–37.

Sakoglu U, Pearlson GD, Kiehl KA, Wang YM, Michael AM, Calhoun VD, 2010 A method for evaluating dynamic functional network connectivity and taskmodulation: application to schizophrenia. Magnetic Resonance Materials in Physics, Biology and Medicine 23, 351–366.

Smith SM, Miller KL, Salimi-Khorshidi G, Webster M, Beckmann CF, Nichols TE, … Woolrich MW, 2011 Network modelling methods for FMRI. Neuroimage 54, 875–891. [PubMed: 20817103]

Sui J, Adali T, Pearlson GD, Calhoun VD, 2009 An ICA-based method for the identification of optimal FMRI features and components using combined group- discriminative techniques. Neuroimage 46, 73–86. [PubMed: 19457398]

Sullivan PF, Kendler KS, Neale MC, 2003 Schizophrenia as a complex trait: evidence from a meta-analysis of twin studies. Archives of general psychiatry 60, 1187–1192. [PubMed: 14662550]

Wang D, Zhou Y, Zhuo C, Qin W, Zhu J, Liu H, …Yu C, 2015 Altered functional connectivity of the cingulate subregions in schizophrenia. Translational psychiatry 5, e575. [PubMed: 26035059]

Wolf DH, Gur RC, Valdez JN, Loughead J, Elliott MA, Gur RE, Ragland JD, 2007 Alterations of fronto-temporal connectivity during word encoding in schizophrenia. Psychiatry Research: Neuroimaging 154, 221–232. [PubMed: 17360163]

Wu L, Eichele T, Calhoun VD, 2010 Reactivity of hemodynamic responses and functional connectivity to different states of alpha synchrony: a concurrent EEG- fMRI study. Neuroimage 52, 1252–1260. [PubMed: 20510374]

Zhu Y, Tang Y, Zhang T, Li H, Tang Y, Li C, …Wang J, 2017 Reduced functional connectivity between bilateral precuneus and contralateral parahippocampus in schizotypal personality disorder. BMC psychiatry 17, 48. [PubMed: 28152990]

Author Manuscript Author Manuscript Author Manuscript Author Manuscript

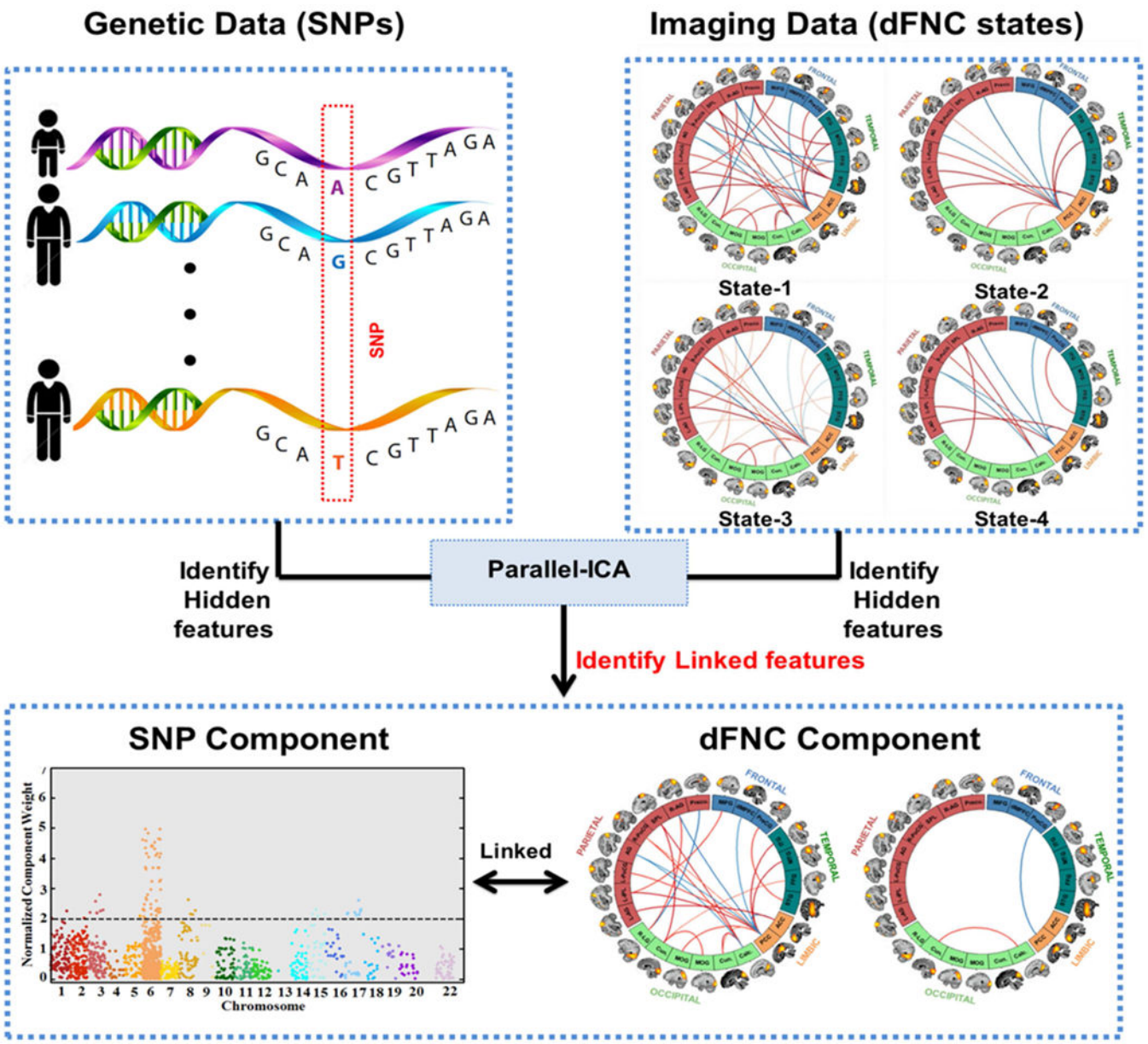

Figure 1: An overview of proposed imaging genetics approach.

Genomic features (preselected SNPs) and imaging features (dynamic connectivity states estimated using sliding-window k-means clustering approach) are used in a parallel independent component analysis (pICA) framework, and the component showing significant association between genomic and imaging features is identified.

Author Manuscript Author Manuscript Author Manuscript Author Manuscript

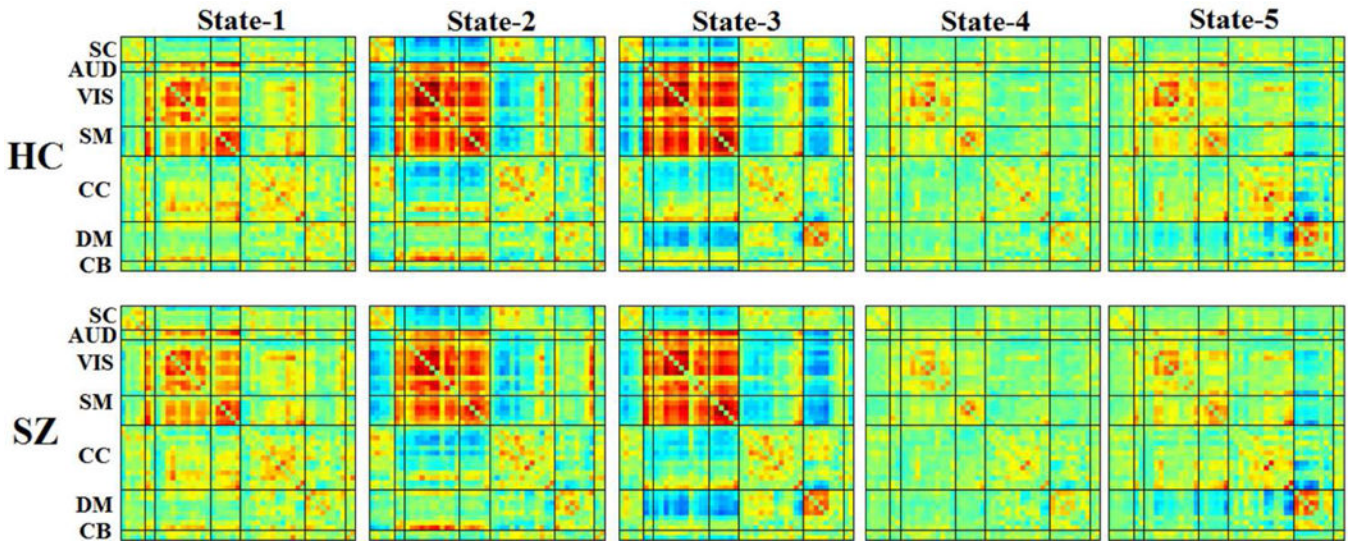

Figure 2: Dynamic connectivity states from clustering approach for k=5.

Group- specific centroids of the dynamic states for healthy (HC) and schizophrenia (SZ) are obtained from k-means clustering.

Author Manuscript Author Manuscript Author Manuscript Author Manuscript

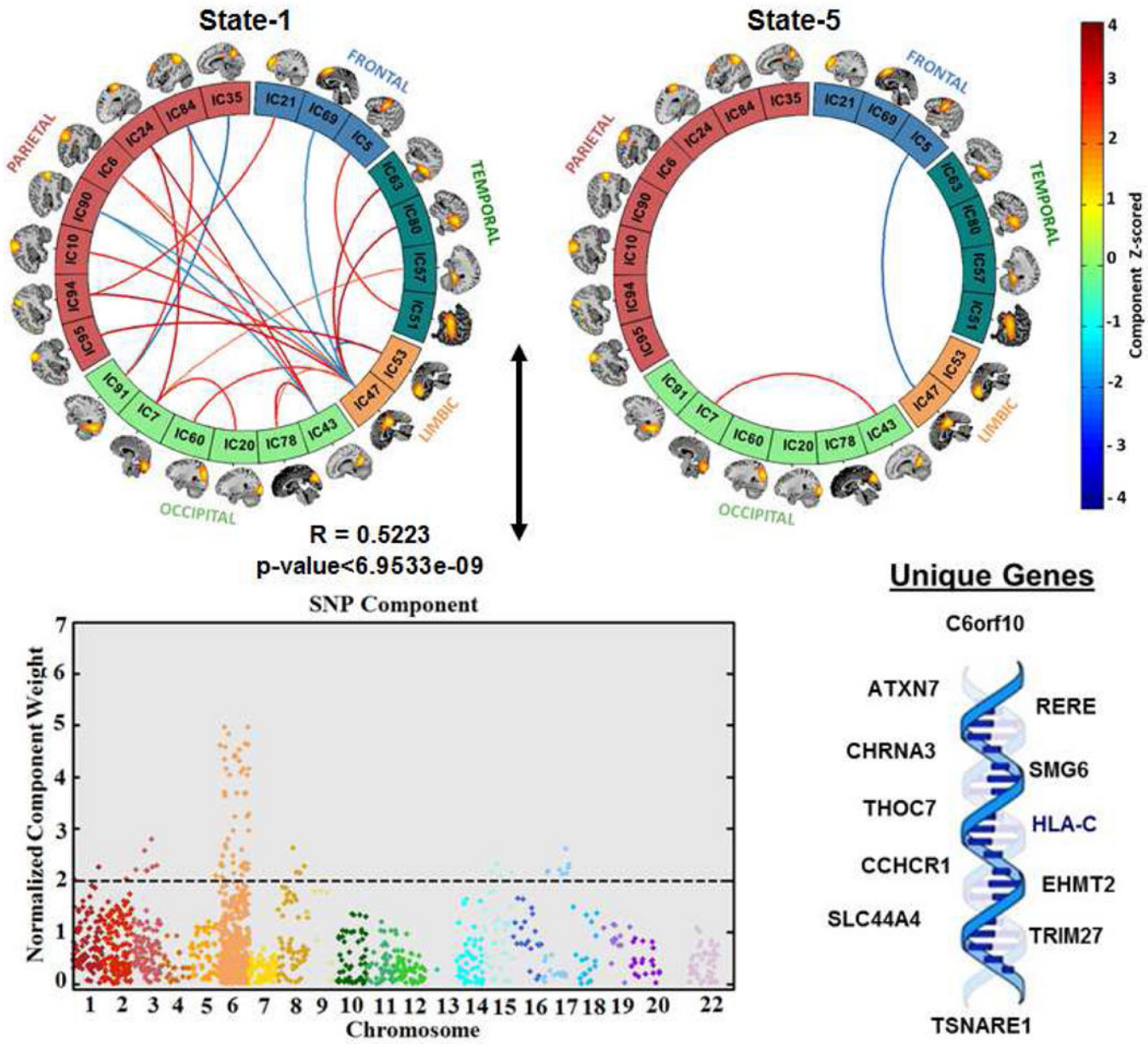

Figure 3: Parallel ICA component.

Results from pICA showing significantly correlated dFNC component (top), and SNP component (bottom). For the dFNC component the significant links (i.e., functional connections with highest connectivity strengths thresholded using **z**-scores of connectivity strengths: |**z**| > 3) and their connectivity strengths for the functional component are shown. For the SNP component, a Manhattan plot highlighting the thresholded SNPs at |**z**| > 2, and the unique genes that these thresholded SNPs are mapped into are shown.

Author Manuscript Author Manuscript Author Manuscript Author Manuscript

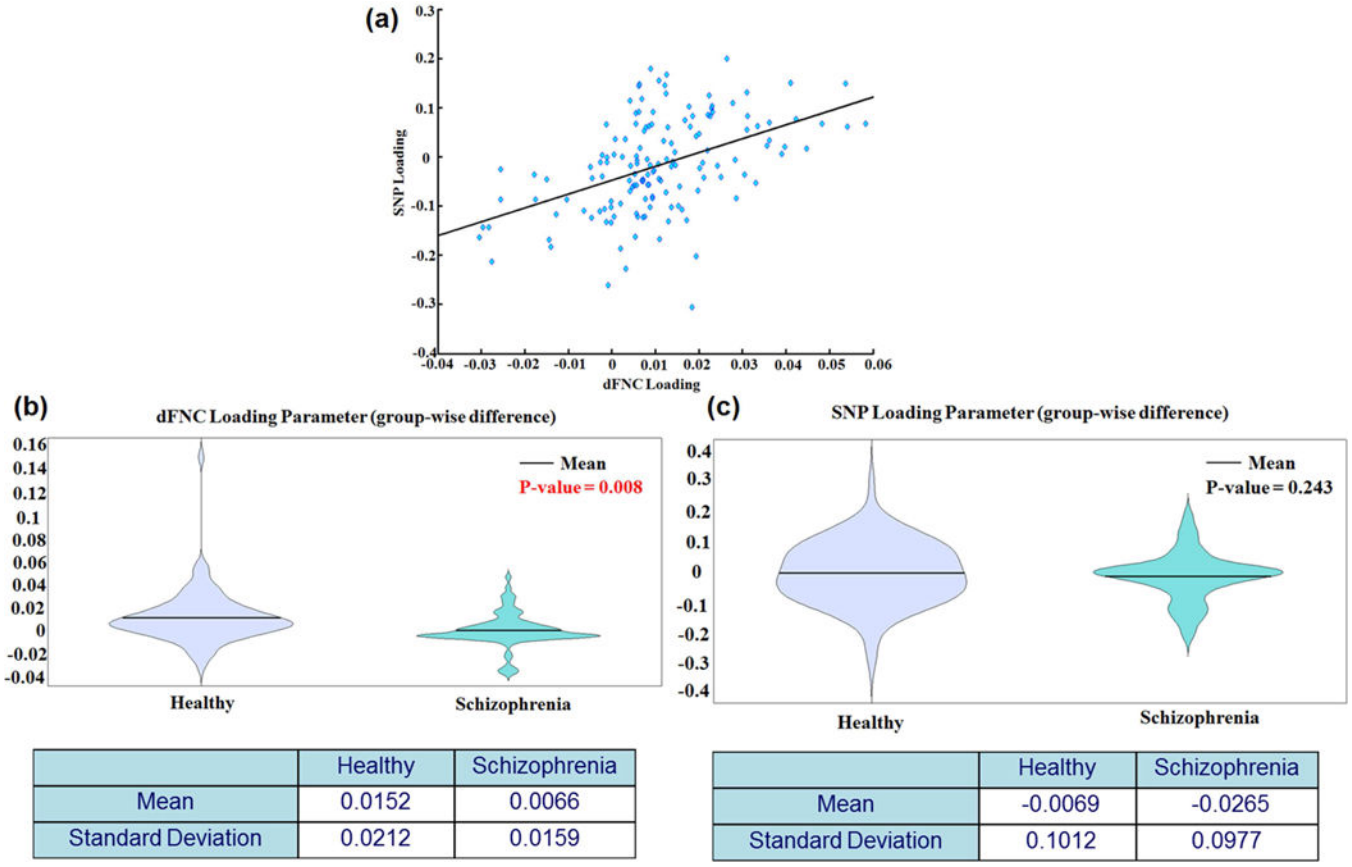

	Healthy	Schizophrenia
Mean	0.0152	0.0066
Standard Deviation	0.0212	0.0159

	Healthy	Schizophrenia
Mean	-0.0069	-0.0265
Standard Deviation	0.1012	0.0977

Figure 4: Loading parameter from the significant parallel ICA component.

Scatterplot showing dFNC loading parameters versus SNP loading parameters from the significant pICA component (top), group-wise violin plots of dFNC loading parameters (middle, left) and SNP loading parameters (middle, right).

Author Manuscript Author Manuscript Author Manuscript Author Manuscript

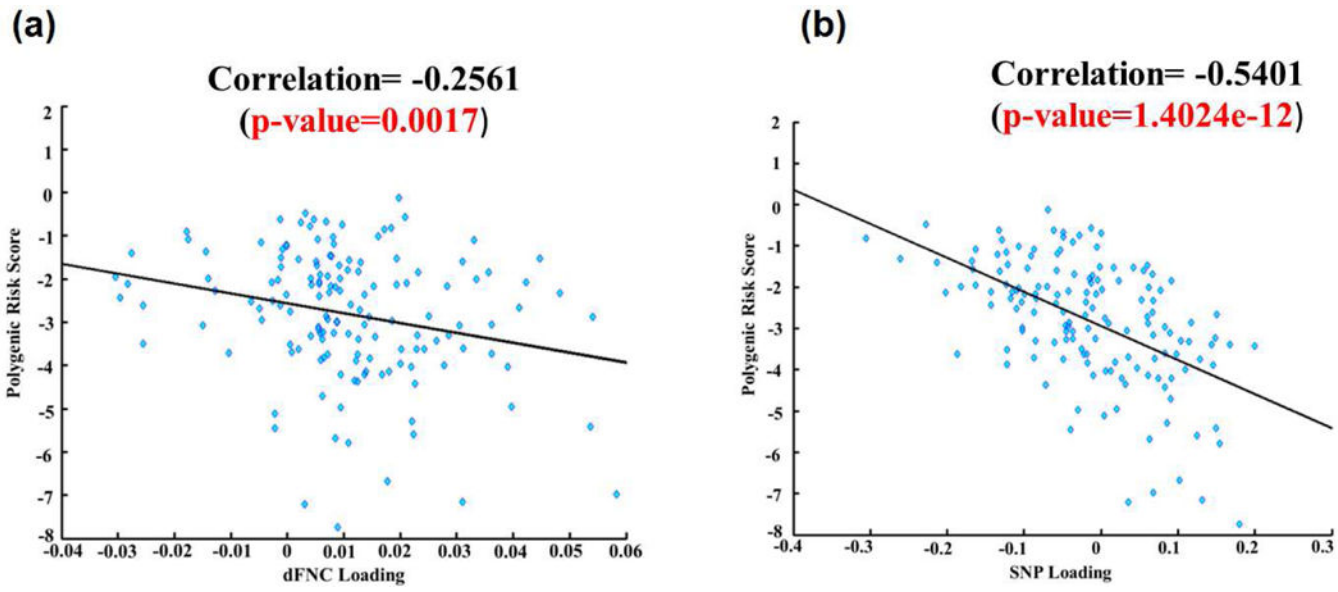

Figure 5: Component loading parameters and polygenic risk scores.

Scatterplots showing polygenic risk scores versus (a) dFNC loading parameters and (b) SNP loading parameter for the significant pICA component.

Author Manuscript

Author Manuscript

Author Manuscript

Author Manuscript

Table 1:

Significant dynamic FNC cells and group-wise occupancy rate across each state

State#	#dFNC Cells	Occupancy (HC/SZ)
1	23	22%/14%
2	0	32%/11%
3	0	20%/18%
4	0	9%/32%
5	2	16%/27%

Author Manuscript

Author Manuscript

Author Manuscript

Author Manuscript

Table 2:

Reactome Pathway Analysis using the top genes

Canonical Pathway	P-value	Gene Name
Neuronal System	0.604202	CHRNA3
Neurotransmitter Receptor Binding And Downstream Transmission In The Postsynaptic Cell	0.313669	CHRNA3
Transmission across Chemical Synapses	0.431053	CHRNA3
Immune System	9.28E-05	HLA-C
Metabolism	0.064322	SLC44A4, ATXN7
Gene Expression	0.866556	EHMT2, THOC7, SMG6

Author Manuscript

Author Manuscript

Author Manuscript

Author Manuscript

Table 3:

Biological functions of the top genes

Functions	P-value	Gene Name
Neurological Disease, Psychological Disorders	4.64E-02	CHRNA3
Hereditary Disorder, Neurological Disease	6.78E-04	ATXN7
Molecular Transport, RNA Trafficking	3.10E-04	SMG6, THOC7
Visual System Development and Function	4.45E-02	ATXN7
Cell Morphology, Embryonic Development	6.76E-03	CCHCR1
Nervous System Development and Function, Tissue Morphology	1.55E-02	ATXN7
Developmental Disorder, Neurological Disease	3.34E-02	SMG6
Immunological Disease	1.08E-02	RERE
Immunological Disease, Inflammatory Disease, Inflammatory Response	6.78E-04	HLA-C

Author Manuscript Author Manuscript Author Manuscript Author Manuscript

Table 4:

Peak activations of ICN spatial maps related to significant links identified from pICA framework. For more information on ICNs, see (Damaraju et cl., 2014).

	BA	Nv	Tmax.	Coordinate
Auditory				
IC51				
R Middle T emporal Gyrus	21	440	32.6	63, −15, −9
L Middle T emporal Gyrus	21	300	30.4	−60, −18, −6
Visual				
IC57				
L Parahippocampal Gyrus	37	234	37.5	−24, −45, −12
R Parahippocampal Gyrus	37	206	39.3	30, −45, −12
IC7				
R Cuneus	17	855	54.4	3, −84, 6
IC20				
R Middle Frontal Gyrus	10	332	31.2	−30, −93, −6
L Superior Frontal Gyrus	10	278	29.4	30, −90, 5
IC78				
R Cuneus	18	949	29	3, −87, 21
IC43				
R Calcarine Gyrus	30	952	23.2	15, −63, 9
IC24				
R Superior Parietal Lobule	7	768	25.3	−32, −88, −1
IC91				
R Lingual Gyrus	19	277	29.9	27, −66, −6
IC60				
R Precuneus	19	357	39.8	30, −78, 33
L Cuneus	19	278	33.6	−27, −78, 27
IC80				
R Middle T emporal Gyrus	22	414	38.4	54, −51, 12
L Middle T emporal Gyrus	22	185	28.1	−54, −51, 9
Sensorimotor				
IC6				
Right Postcentral Gyrus	3	622	39.8	42, −21, 54
IC10				
L Precentral Gyrus	4	598	39.6	−36, −24, 51
IC5				
R Precentral Gyrus	6	328	47.4	54, −6, 27
L Precentral Gyrus	6	288	49.6	−54, −9, 30
Cognitive Control				

Author Manuscript

Author Manuscript

Author Manuscript

Author Manuscript

	BA	Nv	Tmax.	Coordinate
IC63				
L Fusiform Gyrus	37	236	35.6	−42, −57, −12
R Fusiform Gyrus	37	89	28.1	45, −54, −12
IC35				
R Middle Frontal Gyrus	10	332	31.2	33, 54, 12
L Superior Frontal Gyrus	10	278	29.4	−33, 45, 21
IC47				
Cingulate Gyrus	23	621	47.4	0, −36, 27
IC94				
R Inferior Parietal Lobule	40	374	34.9	−42, −42, 45
IC21				
R Middle Frontal Gyrus	10	332	31.2	33, 54, 12
L Superior Frontal Gyrus	10	278	29.4	−33, 45, 21
Default-mode				
IC84				
R Angular Gyrus	40	443	45.8	51, −60, 39
IC90				
R Angular Gyrus	39	213	36.1	45, −75, 30
L Superior Occipital Gyrus	19	89	26.6	−36, −81, 30
IC53				
L Anterior Cingulate Gyrus	32	742	43.5	−3, 48, 12
IC69				
R Medial Frontal Gyrus	8	443	45.8	3,42, 45
IC95				
L Angular Gyrus	40	555	43	−48, −63, 42

BA=Brodmann area; Nv=number of voxels in each cluster; Tmax.=maximum t-statistic in each cluster; Coordinate = max coordinate (mm) in MNI space, following LPI convention.

Author Manuscript Author Manuscript Author Manuscript Author Manuscript

Table 5:

Top 80 SNPs ID, chromosome number (Chr. #) and base position

SNP ID	Chr. #	Base Position
rs10779702	chrl	8423510
rs3765971	chrl	8445360
rs6709720	chr2	57967563
rs832190	chr3	63842629
rs704373	chr3	63867355
rs56293138	chr3	63888935
rs59971314	chr3	63914618
rs7615475	chr3	63926661
rs3774720	chr3	63951765
rs13272	chr3	63986170
rs13160798	chr5	152276252
rs150082944	chr6	28728722
rs115003944	chr6	28734806
rs115544230	chr6	28742340
rs116558610	chr6	28773983
rs148659564	chr6	28817300
rs138562260	chr6	28854772
rs115018585	chr6	28862617
rs115673158	chr6	28877773
rs2233956	chr6	31081205
rs3130566	chr6	31102618
rs114523252	chr6	31116636
rs115997058	chr6	31142265
rs139358712	chr6	31147476
rs150576357	chr6	31149520
rs150602567	chr6	31154434
rs114702079	chr6	31154493
rs116340174	chr6	31161577
rs114974300	chr6	31163638
rs149973721	chr6	31166352
rs115250945	chr6	31178279
rs116311494	chr6	31178328
rs115883612	chr6	31183509
rs141197791	chr6	31184877
rs114272705	chr6	31191070
rs139837897	chr6	31195996
rs115761897	chr6	31197074

Author Manuscript Author Manuscript Author Manuscript Author Manuscript

SNP ID	Chr. #	Base Position
rs114504365	chr6	31200764
rs145495788	chr6	31201357
rs116254022	chr6	31202680
rs114151693	chr6	31220273
rs112684598	chr6	31228634
rs2524108	chr6	31232451
rs114031082	chr6	31237061
rs114700001	chr6	31251477
rs116824795	chr6	31258255
rs115612789	chr6	31271700
rs149248545	chr6	31326324
rs2395475	chr6	31326920
rs2523587	chr6	31327400
rs116778584	chr6	31335901
rs2763981	chr6	31840021
rs652888	chr6	31851234
rs142520578	chr6	31861815
rs114425641	chr6	32200670
rs116153975	chr6	32226126
rs143312186	chr6	32229238
rs150597224	chr6	32237221
rs145499705	chr6	32237260
rs116522184	chr6	32237463
rs115430867	chr6	32247710
rs116105456	chr6	32252507
rs114513253	chr6	32270283
rs116434681	chr6	32298484
rs10957102	chr8	60544006
rs7465167	chr8	143315080
rs8180995	chr8	143326237
rs10875482	chr8	143330385
rs564585	chr15	78886227
rs7359276	chr15	78892661
rs11637630	chr15	78899719
rs8042059	chr15	78907859
rs1532292	chr17	2097483
rs11078865	chr17	2109109
rs9906500	chr17	2129210
rs9893527	chr17	2164210

Author Manuscript

Author Manuscript

Author Manuscript

Author Manuscript

SNP ID	Chr. #	Base Position
rs170044	chr17	2197502
rs216200	chr17	2199846
rs2224770	chr17	2205923
rs391300	chr17	2216258
rs114151693	chr6	31220273